Title	Interplay between quantum criticality and geometric frustration in Fe
Author(s)	Waki, T.; Terazawa, S.; Yamazaki, T.; Tabata, Y.; Sato, K.; Kondo, A.; Kindo, K.; Yokoyama, M.; Takahashi, Y.; Nakamura, H.
Citation	EPL (Europhysics Letters) (2011), 94(3)
Issue Date	2011-05-03
URL	http://hdl.handle.net/2433/141868
Right	© IOP Publishing 2011.
Type	Journal Article
Textversion	author

Interplay between quantum criticality and geometric frustration in Fe_3Mo_3N with stella quadrangula lattice

T. Waki[1] [(a)], S. Terazawa[1], T. Yamazaki[1] [(b)], Y. Tabata[1], K. Sato[2] [(c)], A. Kondo[2], K. Kindo[2], M. Yokoyama[3], Y. Takahashi[4] and H. Nakamura[1] [(d)]

[1] *Department of Materials Science and Engineering, Kyoto University, Kyoto 606-8501, Japan*
[2] *Institute for Solid State Physics, The University of Tokyo, Kashiwa 277-8581, Japan*
[3] *Faculty of Science, Ibaraki University, Mito 310-8512, Japan*
[4] *Graduate School of Material Science, University of Hyogo, Koto Hyogo 678-1297, Japan*

PACS 75.30.Kz – Magnetic phase boundaries
PACS 74.40.Kb – Quantum critical phenomena

Abstract – We propose the η-carbide-type correlated-electron metal Fe_3Mo_3N as a new candidate for testing geometric frustration in itinerant-electron magnets. In this compound, ferromagnetism is abruptly induced from a nonmagnetic non-Fermi-liquid ground state either when a magnetic field (∼14 T) applied to it or when it is doped with a slight amount of impurity (∼5% Co). We observed a peak in the paramagnetic neutron scattering intensity at finite wave vectors, revealing the presence of the antiferromagnetic correlation hidden in the magnetic measurements. It causes a new type of geometric frustration in the *stellla quadrangula* (SQ) lattice of the Fe sublattice, which is a corner-shared lattice of two nested regular tetrahedrons. Although the SQ lattice is one of pyrochlore-derived lattices, we anticipate unique nature of the frustration due to the competition between first- and second-neighbour interactions, J_1 and J_2, possibly of direct exchange type. We propose that the frustrated antiferromagnetic correlation suppresses the ferromagnetic correlation to its marginal point and is therefore responsible for the origin of the ferromagnetic quantum critical behaviour in pure Fe_3Mo_3N.

The geometric frustration in electronic degrees of freedom is a key factor responsible for the suppression of long-range magnetic order that may lead to the realisation of new and exotic quantum phenomena [1]. Although the role of frustration was established in localised electron systems, no consensus has been achieved as far as their role in itinerant electron metals is concerned [2]. One of the reasons for this is the fact that a limited number of materials of this type are available. Y(Sc)Mn_2 [3], β-Mn [4], LiV_2O_4 [5], etc. are some of the known examples, whose electronic quasiparticle mass is commonly enhanced but the manner in which it is enhanced is still under debate. To resolve this issue, it is essential that we find other materials of a similar nature, metallic lattices with the appropriate interatomic distance which enables both direct exchange coupling between magnetic atoms and strong electron correlation. The magnetic lattice of both Y(Sc)Mn_2 and LiV_2O_4 is the so-called pyrochlore lattice, which is a typical highly frustrated lattice. β-Mn has the three-dimensionally twisted kagome lattice. In this letter, we propose the η-carbide-type transition metal compound as a new candidate for testing geometric frustration in metallic magnets; the η-carbide-type structure (prototype: Fe_3W_3C, space group: $Fd\bar{3}m$) includes the *stella quadrangula* (SQ) lattice (Wyckoff positions 16*d* and 32*e*) [6], which is a corner-shared network of stellate (tetra-capped) tetrahedrons (see Fig. 1). In an SQ as a unit, a small regular tetrahedron at 32*e* is nested in each 16*d* tetrahedron having the same centre of gravity. Furthermore, direct coupling is expected at the relatively short Fe-Fe bonds. The only 16*d*-site network is the pyrochlore lattice, but the nature of the magnetic interaction in the SQ lattice is expected to be different as mentioned below, if we consider only the near neighbour interactions.

[(a)] E-mail: takeshi.waki@kx7.ecs.kyoto-u.ac.jp
[(b)] Present address: Institute for Solid State Physics, The University of Tokyo, Kashiwa 277-8581, Japan
[(c)] Present address: Ibaraki National College of Technology, Department of Natural Science 866 Nakane, Hitachinaka 312-8508, Japan
[(d)] E-mail: h.nakamura@ht8.ecs.kyoto-u.ac.jp

Even though η-carbide-type transition-metal compounds have been known for a long time as impurities in steel and refractory and hard materials, as well as promising candidates for catalysts, etc. [7], their quantum physical properties have been less studied thus far (as an exception, see [8]). We have recently reported that Fe_3Mo_3N with the η-carbide-type structure [9] exhibits a non-Fermi liquid (NFL) behaviour near the ferromagnetic quantum critical point (QCP) under ambient pressure [10], which is different from the findings of literatures published previously [11, 12]; C/T (C: specific heat, T: temperature) shows a $-\log T$ divergence and reaches 128 mJ/(f.u.mol K^2) at 0.5 K, and the resistivity shows a $T^{5/3}$ dependence. Fe_3Mo_3N is a one of the ideal Fe-based materials exhibiting NFL behavior [13, 14].

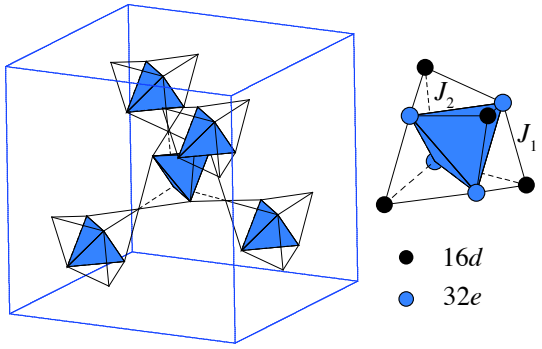

Fig. 1: (colour online) Schematic view of the *stella quadrangula* (SQ) lattice, which is a corner-shared network of stellate (tetra-capped) tetrahedra. The unit, a *stella quadrangula*, consists of two nested regular tetrahedra made of 16d and 32e sites in the space group $Fd\bar{3}m$ with the same centre of gravity. The network of only the 16d site is the so-called pyrochlore lattice, but in the SQ lattice, the first-neighbour 16d-32e and second-neighbour 32e-32e interactions are expected to be dominant comparing with the pyrochlore-type 16d-16d interaction.

The susceptibility χ of Fe_3Mo_3N obeys the Curie-Weiss (CW) law at high temperatures (effective moment $p_{\rm eff}$ = 2.14 $\mu_{\rm B}$/Fe, Weiss temperature θ = 2 K) and exhibits a broad maximum at ∼75 K [10]. No field-cool effect was observed in $\chi(T)$. Because the $\chi(T)$ maximum is commonly observed among exchange-enhanced Pauli paramagnetic metals undergoing itinerant-electron metamagnetism (IEM) [15], the application of a high magnetic field to Fe_3Mo_3N may yield interesting results. IEM of Fe_3Mo_3N is also fascinating related with the recent interest in the phase diagram in the vicinity of ferromagnetic-QCP and tuning of quantum criticality [16]. While we have detected the IEM at ∼14 T, it is somewhat different from a typical IEM [15]. In order to determine the reason for this difference, impurity doping (Co for Fe) and inelastic neutron scattering measurements of Fe_3Mo_3N were performed. In this letter, we discuss the characteristics of the SQ lattice as a new geometrically frustrated system, and we use this model to explain the absence of long-range order in pure Fe_3Mo_3N in spite of the strong electron correlation.

Polycrystalline samples of $(Fe_{1-x}Co_x)_3Mo_3N$, where $0 \le x \le 1$, were synthesised by a solid-state reaction of a mixture of transition metal oxides in a H_2-N_2 mixed gas stream [17]. Fe_2O_3, Co_3O_4, and MoO_3 were mixed in a molar ratio of $(1-x)/2 : x/3 : 1$ and placed in a silica tube; and the mixture was then fired in a gas stream of N_2 containing 10% H_2 at 700°C for 48 h followed by heat treatment at 1000°C for 48 h. In order to homogenise the samples, the heat treatment, interspersed with intermediate grinding, was repeated at least four times, resulting in a systematic variation in the magnetism against x, which is not in accordance with the literature data [12]. The magnetisation M at low fields was measured in the range from 2 to 300 K and up to 5.5 T using a SQUID magnetometer MPMS (Quantum Design) equipped in the LTM centre, Kyoto University. The high-field magnetisation for field strengths up to 54 T was measured for pure Fe_3Mo_3N using a pulse magnet equipped in ISSP at 4.2–100 K. Polycrystalline powder was filled into a cylindrical polyethylene tube that measured 6 mm in length and 2.5 mm in diameter. For the neutron scattering experiments, approximately 20 g of the powder was packed into a vanadium tube with a diameter of 20 mm. A triple-axis spectrometer ISSP-HER installed at the C1-1 cold neutron guide of the research reactor JRR-3M at Japan Atomic Energy Agency (JAEA), Tokai, was employed. All measurements were performed at a fixed final wave vector $k_{\rm f}$ = 1.45 Å^{-1}, with a collimation sequence of guide-40′-open-open, and with a horizontal focusing analyser. The energy resolution was estimated to be 0.22 meV at zero energy transfer.

Figure 2 shows the results of the high-field magnetisation measurements. The signal from the pulse magnet corresponding to dM/dH (at 4.2 K) is plotted against the external magnetic field H in the inset of Fig. 2(a). dM/dH shows diverging behaviour at ∼14 T, corresponding to a sharp jump in the M-H curve, which was obtained by integrating dM/dH. The metamagnetic fields $H_{\rm C}$ are different for the field-increasing and decreasing processes because of the first-order transition, although the difference (hysteresis width) ΔH is much smaller (0.56 T at 4.2 K) than that for a typical IEM [15]. ΔH decreases with temperature and vanishes at $T_{\rm CM} \simeq 42$ K (Fig. 2(c)), which is the temperature at which the first-order IEM disappears. The critical field $H_{\rm C}$ at $T_{\rm CM}$ was estimated as 15.8 T. The increase in $H_{\rm C}$ is roughly proportional to T^2 up to $T_{\rm CM}$ (Fig. 2(b) closed circles), as commonly observed in IEM [15]. The magnetisation jump at $H_{\rm C}$ is reduced on approaching $T_{\rm CM}$. In the field-increasing process, a small step was observed at a field (defined as $H_{\rm E}$) slightly greater than $H_{\rm C}$ as seen in Fig. 2(a). $H_{\rm E}$ decreases gradually with temperature and disappears at ∼20 K (Fig. 2(b) open circles). The magnetisation jump is sharp unlike that observed in other IEMs [15] and rather similar to that of a spin flip in a localised spin system. This is in contrast to the fact that

another η-carbide-type compound Co_3Mo_3C shows rather gradual IEM [18]. Successive magnetic transitions in the magnetic field are frequently observed in local spin systems; however, they are unlikely to be a part of a conventional IEM with uniform spin polarisation, thus suggesting the presence of competing interactions or multiple order parameters. Observations of possible magnetovolume coupling and change in the lattice symmetry at H_C would be helpful to figure out the mechanism of the transition.

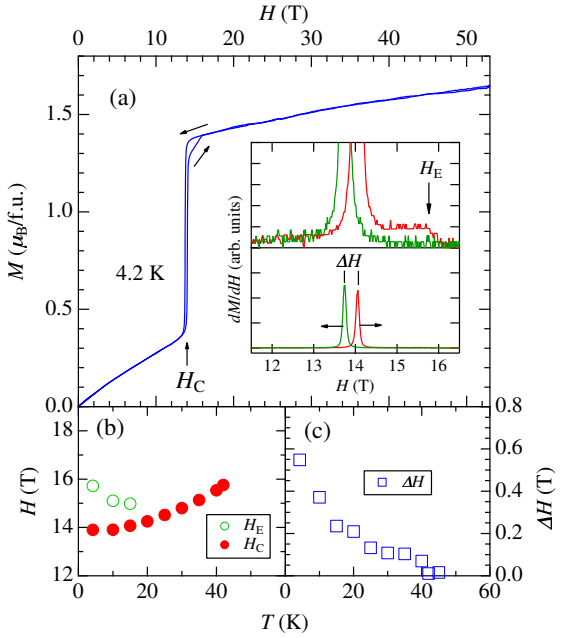

Fig. 2: (colour online) (a) High-field magnetisation curve of Fe_3Mo_3N at 4.2 K. The inset shows dM/dH in both field-increasing and decreasing processes. The top half of the inset shows a magnified version of the image in the bottom half. (b) Temperature dependences of the metamagnetic field H_C (average value of field-increasing and decreasing processes, closed circles) and the field of the small anomaly in the field-increasing process, H_E (open circles). (c) Temperature dependence of the hysteresis width ΔH.

The effect of impurity doping was investigated by replacing Co with Fe. We have successfully synthesised a solid solution between Fe_3Mo_3N and Co_3Mo_3N. One of the end compounds, Co_3Mo_3N, shows a weakly temperature-dependent Pauli paramagnetic behaviour [18]. The lattice parameter at room temperature was found to vary linearly with the Co fraction x (Vegard's law), which is in good accordance with the literature data [12]. With the Co doping, we observed the onset of ferromagnetic order, despite the fact that both end compounds have nonmagnetic ground states. As a typical example, the magnetic data of $(Fe_{0.8}Co_{0.2})_3Mo_3N$ are presented in Figs. 3(a) and (b). At high temperatures, $\chi(T)$ roughly follows the CW law, but in fact, $1/\chi$ is not linear to temperature but convex upward. This is probably due to both Fe and Co with different roles contribute to $\chi(T)$. Here we formally analysed $\chi(T)$ assuming the CW law with a temperature-independent term χ_0. Thus the effective paramagnetic moment $p_{\rm eff}$ and the Weiss temperature θ were estimated as 2.15 $\mu_B/3d$-atom and 22.0 K, respectively. As shown in Fig. 3(a), the Arrott plot (M^2 against H/M plot) shows good linearity and intersects the vertical axis below 22 K, indicating the occurrence of spontaneous magnetisation p_s ($= 0.23\ \mu_B/3d$-atom at 1.8 K) below the Curie temperature $T_C = 22$ K. The value of $p_{\rm eff}/p_s$ is much larger than unity, as is characteristic of a typical weak itinerant electron ferromagnet. Similar analyses were carried out for other specimens. Estimated $p_{\rm eff}$, θ and χ_0 are plotted as functions of x in Figs. 3(c) and (d). $p_{\rm eff}$ per $3d$ atom is nearly independent of x, and θ, which is nearly 0 at $x \sim 0$, once takes positive values equal to T_C and turns to be negative at higher x. The latter fact suggests the evolution of exchange interaction among magnetic atoms. However, note that these values were estimated only tentatively by assuming the modified CW law including temperature-independent χ_0. As noticed from the rapid increase of χ_0 with x, the value of θ as well as accidentally x-independent p_s seem to be less significant particularly at the Co-rich side.

In Fig. 4, the values of T_C are plotted against x together with the contour map of M/H to visualize the magnetic phase diagram. Appearance of internal field below T_C was confirmed for all ferromagnetic compounds by observing additional broadening of ^{57}Fe Mössbauer spectra [19]. Spontaneous moments p_s per $3d$ atom (Fe+Co) is plotted against x in the inset of Fig. 4. p_s per Fe atom, estimated by assuming that Fe atoms bear all the moment, is also plotted in the same figure. Nearly concentration independent p_s/Fe except low- and high-x ends is consistent with internal fields estimated in the Mössbauer analyses, and hence justify the assumption that the Fe sites are responsible for the principal part of the magnetism. For the sample with $x \leq 0.1$, we have performed high-field magnetisation measurements and estimated H_C (at 4.2 K) and T_{CM}, which are also plotted in Fig. 4. Note that the ferromagnetic samples with $0.05 \leq x \leq 0.1$ show also metamagnetic transitions. The characteristics of this phase diagram are as follows. A ferromagnetic phase appears by slight doping ($x < 0.05$). With an increase in x, T_C increases rapidly up to a maximum at $x \sim 0.2$ and decreases almost linearly after the maximum up to $x \sim 0.7$. The linear decrease of T_C can be interpreted as a consequence of dilution of magnetic Fe atoms. The region of the induced ferromagnetic phase is strongly asymmetric unlike the impurity induced ferromagnetic phase observed for the itinerant-electron metamagnetic system YCo_2 [20]. It also should be noted that the metamagnetic field H_C, which corresponds to the magnetic interaction, increases almost linearly with decreasing x. T_{CM} is the highest at $x = 0$ and decreases rapidly to zero at the critical phase boundary at $x = 0.05$. These results suggest that long-range ferromagnetism is suppressed particularly at $x \sim 0$,

in spite of stronger exchange enhancement expected also from the larger lattice volume at $x \sim 0$. In the previous article [12], remarkable scattering of T_C ranging from 0 to 45 K, and hence no correlation between T_C and x have been reported in contrast to our systematic variation of T_C. Since raw magnetic data are limited in the literature, it seems to be difficult to comment on the origin of this considerable discrepancy. One of possible reasons is the difference in heterogeneity of samples or the extent of atomic clustering at the 16*d* and 32*e* sites, which would depends on the condition of heat treatments.

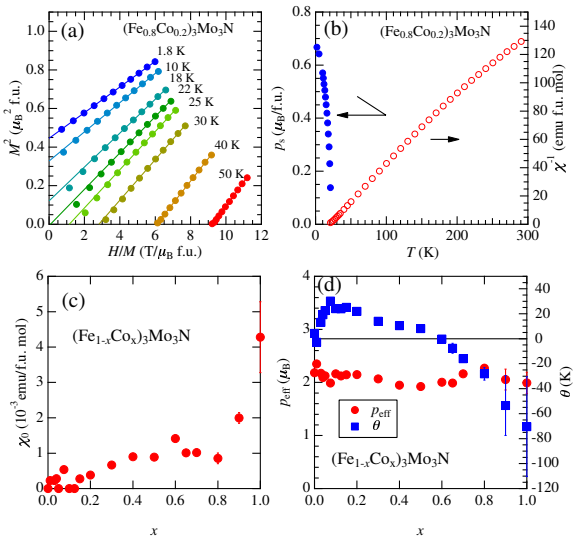

Fig. 3: (color online) (a) Arrott plots of $(Fe_{0.8}Co_{0.2})_3Mo_3N$. (b) Temperature dependences of inverse susceptibility and spontaneous magnetisation (estimated from the Arrott plot) of $(Fe_{0.8}Co_{0.2})_3Mo_3N$. (c) χ_0 plotted against x. (d) p_{eff} per 3*d* atom and θ plotted against x.

To obtain information on the magnetic interactions in Fe_3Mo_3N, inelastic neutron scattering experiments were performed with the powder; unfortunately, single crystals have not been obtained. Figure 5(a) shows the wave number (K) dependences of quasi-elastic neutron scattering measured at 5.5 K and at energy transfers $E = 1$ and 2 meV. Relatively strong scattering was observed at finite K, and likely to be centered at $K \sim 2$ in the reciprocal lattice unit (r.l.u.) at the lower energy transfer. Due to the limitation of the machine time, we could measured E-spectra only at three K points, which are shown in Fig. 5(b) and fitted with a Lorentzian quasi-elastic scattering function. The spectral width, i.e., the characteristic energy of spin fluctuations increases with K as 0.4, 0.3 and 0.9 meV for $K = 1.22$, 1.78, and 2.83 r.l.u., respectively. The E-integrated scattering function $S(K)$ are estimated at the three K points, and plotted in Fig. 5(c). Referring to the K spectra in Fig. 5(a) and assuming monotonic K dependence of the characteristic energy of spin fluctuations, this result suggests the presence of a broad peak

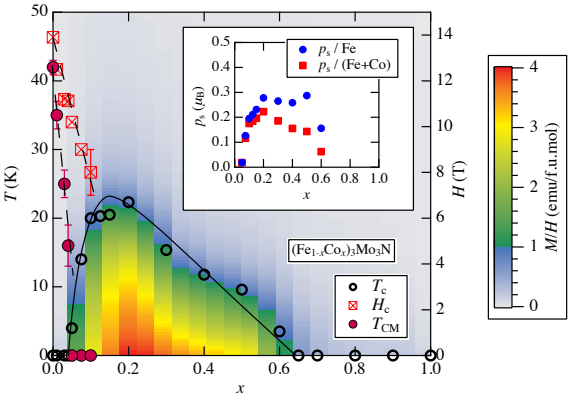

Fig. 4: (colour online) Magnetic phase diagram of the $(Fe_{1-x}Co_x)_3Mo_3N$ system. T_C (open circles) were determined from Arrott plots. T_{CM} (closed circles) is the temperature where the first-order metamagnetism disappears. H_C (checked squares) is the metamagnetic field at 4.2 K. Contour plot of M/H is also shown. Dashed and solid curves are guide for eyes. The inset shows concentration dependences of the spontaneous magnetic moment per Fe or 3*d* atom.

in $S(K)$ at finite K, suggesting the presence of antiferromagnetic spin correlation with a short correlation length together with the ferromagnetic correlation that was detected from macroscopic measurements.

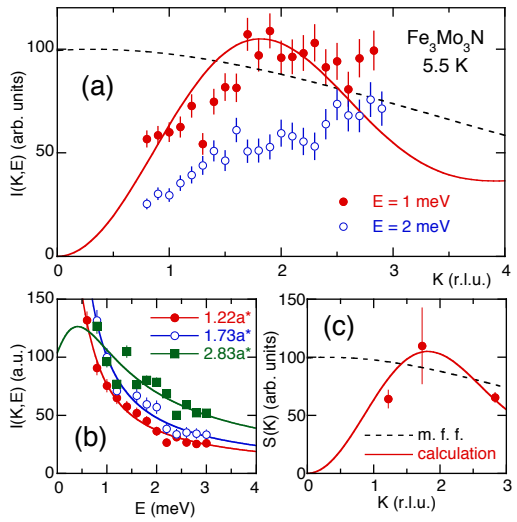

Fig. 5: (colour online) (a) Wave number (K) dependences of quasi-elastic neutron scattering of Fe_3Mo_3N at 5.5 K for energy transfers of $E = 1$ and 2 meV. K is in the reciprocal lattice unit (r.l.u.). (b) E-scan spectra at 5.5 K and at $K = 1.22$, 1.73, and 2.83 r.l.u. Solid curves represent the best fits to the Lorentzian quasi-elastic scattering function. (c) E-integrated scattering function $S(K)$. The solid curve represents $S(K)$ calculated for the SQ lattice (see text). The broken curve represents the K dependence of the squared magnetic form factor for Fe^{3+}. The same carves are also drawn in (a) as references.

Band calculations of Fe_3Mo_3N told us that Fe 3*d* bands

are main contribution to the density of states at the Fermi level, $D(E_F)$, and that Fe atoms at the two different crystallographic sites contribute nearly equally to $D(E_F)$ [10]. In the following, we neglect the effect of Mo $4d$ bands and consider only the Fe sublattice for the sake of simplicity. Let us understand the geometrical characteristics of the Fe sublattice, i.e., the SQ lattice on the basis of the Heisenberg model. Although Fe_3Mo_3N appears to behave like an itinerant electron magnet, we believe that its spin density is relatively localised at the atomic site, as deduced from the strong electron correlation. The SQ lattice consists of $16d$ and $32e$ sites arranged in the $Fd\bar{3}m$ space group. In actual η-carbide-type compounds, the nearest-neighbour (nn) and next-nearest-neighbour (nnn) distances are close and become exactly the same when $z = 0.3$, where z is the coordinate of the $32e$ site (z, z, z). Experimentally, $z = 0.2937$ [9] and similar values [21, 22] have been reported for Fe_3Mo_3N, where the nn $16d$-$32e$ distance is 2.387 Å and nnn $32e$-$32e$ distance is 2.549 Å at room temperature. These distances are close to interatomic distances of correlated electron intermetallics such as $Y(Sc)Mn_2$.

Here, we consider only these nn and nnn interactions, namely, J_1 and J_2 (see Fig. 1), respectively, and neglect the interactions of the neighbours located further along. Note that, if we pick up only the $16d$ atoms, the network is the pyrochlore lattice, which is a typical highly frustrated lattice. In the SQ lattice, however, the interaction between $16d$ atoms would be minor because we expect direct exchange coupling between first- and second-neighbours but the distance between $16d$ atoms ($\simeq 3.92$ Å) is likely to be too large to form direct coupling. The signs of J_1 and J_2 are likely to vary because, empirically, both the ferromagnetic and the antiferromagnetic states appear in doped Fe-based η-carbide-type compounds [8]. First, let us understand the nature of an isolated SQ. In an extreme case, with $J_1 < 0$ and $J_2 = 0$, the SQ is not frustrated because the antiferromagnetic spins can be alternately assigned to the eight atoms. Needless to say, the same is the case for $J_1 > 0$ and $J_2 = 0$. On the other hand, when $J_1 = 0$ and $J_2 < 0$, the isolated $32e$ tetrahedron is a typical frustrated unit. These facts suggest that the SQ is frustrated only when J_2 is negative and dominant. It should be noted that this is true not only when $J_1 < 0$ but also when $J_1 > 0$. To verify whether this is true for an infinite SQ lattice, we calculated the dispersions of the Fourier transform of the exchange integral matrix $J(q)$ among 12 Fe atoms in a unit cell by assuming various J_1/J_2 ratios. Two typical results are shown in Fig. 6. A flat dispersion is found along the highest branch when J_1 is not dominant (Fig. 6(a)), suggesting the degeneracies of the ground state, i.e., the presence of geometric frustration [23]. On the other hand, $J(q)$ takes a maximum at the Γ point, where the magnitude of J_1 is sufficiently larger than that of J_2 (Fig. 6(b)), indicating that J_1 tends to release the frustration. We confirmed that similar dispersions were obtained independent of the sign of J_1. Thus, the SQ lattice is a unique frustrated system in which frustration is controlled by the $|J_1|/J_2$ ratio but not affected by the sign of J_1 and discriminated from other typical frustrated lattices [24]. In the pyrochlore lattice, the magnetic ground state is independent of J_1 as well, but the introduction of J_2 releases the frustration at least partially [25]

The anomalous magnetism of Fe_3Mo_3N can be easily understood on the basis of these characteristics. The experimental results indicate the coexistence of the ferromagnetic and the antiferromagnetic interactions, which are formally denoted as J_1 and J_2, respectively, as one of the simplest possibilities. The suppression of long-range order in pure Fe_3Mo_3N is due to the frustration in the SQ lattice (J_2 dominant case). In other words, the frustrated antiferromagnetic interaction suppresses the ferromagnetic correlation to its marginal point. Metamagnetism can be interpreted as the transition to the J_1 dominant state, assisted by the external field. The onset of static magnetism by slight doping is one of common features of a frustrated system. It is not surprising that the ferromagnetic order is stabilised when the F interaction coexists with the antiferromagnetic interaction. We have tentatively calculated the spin correlation function $S(K)$ for the SQ lattice, assuming (1) $J_1 > 0$ and dominant $J_2 < 0$, (2) 2 up and 2 down spins in the $32e$ tetrahedron, (3) an up spin at a $16d$ site when the neighbouring $32e$ spins are 2 up and 1 down, and vice versa, (4) no correlation between different SQs, and (5) the magnetic form factor of Fe^{3+}. Some of these assumptions may not be valid for the actual case, but have been made for the sake of simplicity. $S(K)$ thus calculated is illustrated by the solid curve in Fig. 5(c). Although we have only three experimental points to be compared with the calculation, by referring to the K spectra in Fig. 5(a), the agreement is likely to be reasonable, indicating that our model is consistent with the experimental results. Here we have applied the localised moment scheme simply because there is no adequate way to describe the frustration in the itinerant electron system. We have to reconcile the Heisenberg frustration and the electron itinerancy in further studies.

In summary, we found a steep metamagnetic transition in the η-carbide-type Fe-based compound Fe_3Mo_3N from the nonmagnetic NFL near ferromagnetic-QCP to a field-induced ferromagnetic state, and we established a magnetic phase diagram of the $(Fe_{1-x}Co_x)_3Mo_3N$ system, where the ferromagnetic order is stabilised by a slight doping of the nonmagnetic element. Neutron scattering measurements suggested that the antiferromagnetic and the ferromagnetic correlations coexist in Fe_3Mo_3N. We proposed that the SQ lattice is a new geometrically frustrated system, in which the ferromagnetic and the antiferromagnetic interactions compete to select frustrated and non-frustrated states. Note that the SQ lattice is a derived form from the highly frustrated pyrochlore lattice, but our model of the geometric frustration is essentially different from that for the pyrochlore lattice. We applied this model to explain the suppression of long-

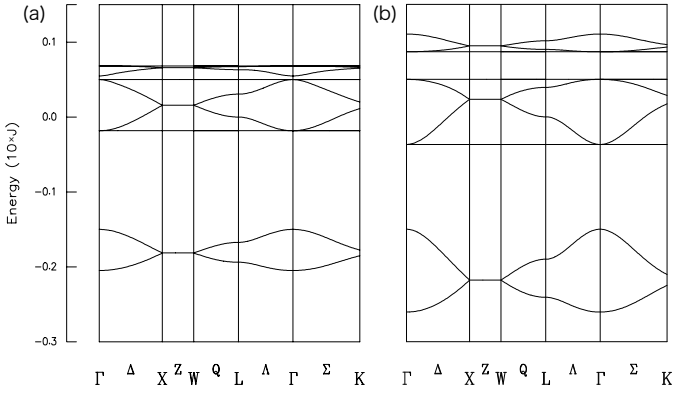

Fig. 6: Typical dispersion curves of $J(q)$ calculated for the SQ lattice with negative J_2. (a) J_2-dominant ($|J_1|/J_2 = -0.5$) and (b) J_1-dominant (-0.8) cases. The results do not depend on the sign of J_1. In these calculations, $z = 0.2937$ was used as the coordinate of $32e$, and the boundary of these states appears between $|J_1|/J_2 = -0.6$ and -0.8.

range order in pure Fe_3Mo_3N. In other words, the emergence of the ferromagnetic-QCP is interpreted as being the result of frustration. Although a number of η-carbide-type transition-metal compounds are known to exist, their quantum physical properties have been less studied. In addition, we can design various types of metallic magnets by selecting species of transition metals and site occupation. We believe that these compounds are good candidates for testing geometric frustration in metallic magnets and searching for new and exotic quantum phenomena.

* * *

The authors thank H. Kobayashi and S. Ikeda at University of Hyogo for the collaboration in Mössbauer analyses. This study was supported by a Grant-in-Aid for Scientific Research on Priority Areas "Novel States of Matter Induced by Frustration" (19052003), a Grant-in-Aid for the Global COE Program, "International Centre for Integrated Research and Advanced Education in Materials Science," and a Grant-in-Aid for Young Scientists (B) 21760531 from the Ministry of Education, Culture, Sports, Science and Technology of Japan.

REFERENCES

[1] for example, Moessner R. and Ramirez A. P., *Physics Today*, **59** (2006) 24-29
[2] Lacroix C., *J. Phys. Soc. Jpn.*, **79** (2010) 011008
[3] Shiga M., Fujisawa K. and Wada H., *J. Phys. Soc. Jpn.*, **62** (1993) 1329-1336; Ballou R., Lelièvre-Berna E. and Fåk B., *Phys. Rev. Lett.*, **76** (1996) 2125-2128
[4] Nakamura H., Yoshimoto K., Shiga M., Nishi M. and Kakurai K., *J. Phys.: Condens. Matter*, **9** (1997) 4701-4728
[5] Kondo S., Johnston D. C., Swenson C. A., Borsa F., Mahajan A. V., Miller L. L., Gu T., Goldman A. I., Maple M. B., Gajewski D. A., Freeman E. J., Dilley N. R., Dickey R. P., Merrin J., Kojima K., Luke G. M., Uemura Y. J., Chmaissem O. and Jorgensen J. D., *Phys. Rev. Lett.*, **78** (1997) 3729-3732
[6] Nyman H., Andersson S. and O'Keeffe M., *J. Solid State Chem.*, **26** (1978) 123-131
[7] for example, Toth L. E., *Transition Metal Carbides and Nitrides* (Academic Press, New York) 1971; Jacobsen C. J. H., *Chem. Commun.*, (2000) 1057-1058
[8] Sviridov L. A., Battle P. D., Grandjean F. Long G. J. and Prior T. J., *Inorg. Chem.*, **49** (2010) 1133-1143
[9] Bem D. S., Gibson C. P. and Loye H.-C. zur, *Chem. Mater.*, **5** (1993) 397-399
[10] Waki T., Terazawa S., Tabata Y., Oba F., Michioka C., Yoshimura K., Ikeda S., Kobayashi H., Ohoyama K. and Nakamura H., *J. Phys. Soc. Jpn.*, **79** (2010) 043701
[11] Panda R. N. and Gajbhiye N. S., *J. Alloys Compd.*, **256** (1997) 102-107
[12] Prior T. J. and Battle P. D., *J. Mater. Chem.*, **14** (2004) 3001-3007
[13] Brando M., Duncan W. J., Moroni-Klementowicz D., Albrecht C., Grüner D., Ballou R. and Grosche F. M., *Phys. Rev. Lett.*, **101** (2008) 026401
[14] Holmes A. T., Jaccard D., Behr G. Inada Y. and Onuki Y., *J. Phys.: Condens. Matter*, **16** (2004) S1121-S1127
[15] for example, Goto T., Fukamichi K. and Yamada H., *Physica B*, **300** (2001) 167-185; Fukamichi K., *Handbook of Advanced Magnetic Materials*, Vol. **2**, edited by Lie Y., Sellmyer D. J. and Shindo D. (Springer, New York) 2006, sect. 7; Yamada H., *Phys. Rev. B*, **47** (1993) 11211-11219
[16] for example, Löhneysen H. v., Rosch A., Vojta M. and Wŀfle P., *Rev. Mod. Phys.*, **79** (2007) 1015-1075; Pfleiderer C., Julian S. R. and Lonzarich G. G., *Nature*, **414** (2001) 427-430; Grigera S. A., Perry R. S., Schofield A. J., Chiao M., Julian S. R., Lonzarich G. G., Ikeda S. I., Maeno Y., Millis A. J., and Mackenzie A. P., *Science*, **294** (2001) 329-332
[17] Prior T. J. and Battle P. D., *J. Solid State Chem.*, **172** (2003) 138-147
[18] Waki T., Umemoto Y., Terazawa S., Tabata Y., Kondo A., Sato K., Kindo K., Alconchel S., Sapiña F., Takahashi Y. and Nakamura H., *J. Phys. Soc. Jpn.*, **79** (2010) 093703
[19] Ikeda S., Kobayashi H., *et al.*, *unpublished data*
[20] Yoshimura K. and Nakamura Y., *Solid State Commun.*, **56** (1985) 767-771
[21] Alconchel S., Sapiña F., Beltrán D. and Beltrán A., *J. Mater. Chem.*, **8** (1998) 1901-1909
[22] Jackson S. K., Layland R. C. and Loye H.-C. zur, *J. Alloys Compd.*, **291** (1999) 94-101
[23] for example, Harris A. B., Kallin C. and Berlinsky A. J., *Phys. Rev. B*, **45** (1992) 2899-2919; and [25]
[24] for example, *Frustrated Spin Systems*, edited by Diep H. T. (World Scientific, Singapore) 2004, sect. 4
[25] Reimers J. N., Berlinsky A. J. and Shi A.-C., *Phys. Rev. B*, **43** (1991) 865-878